IN SITU MONITORING OF CAUTERIZATION WITH A BIOPSY NEEDLE USING IMPEDANCE CHARACTERISTICS OF EMBEDDED PIEZOTHERMAL ELEMENTS

Karthik Visvanathan[1*], Tao Li[2] and Yogesh B. Gianchandani[1,2]

[1]*Department of Mechanical Engineering, University of Michigan, Ann Arbor, USA*

[2]*Department of Electrical Engineering and Computer Science, University of Michigan, Ann Arbor, USA*

ABSTRACT

This paper presents a method for monitoring biological tissue cauterization using the variation in the electromechanical impedance characteristics of the piezothermal heating elements used for tissue ablation. Piezoelectric ultrasonic heaters microfabricated from lead zirconate titanate (PZT) with 200 µm diameter and 100 µm thickness are embedded in a 20-gauge biopsy needle. A modified Butterworth-Van-Dyke circuit is used to model the variation in impedance characteristics of the PZT before and after cauterization. After tissue cauterization, the fundamental anti-resonance frequency and the peak impedance magnitude decrease by 0.6 MHz and 900 ohms, respectively.

KEYWORDS: Cauterization, impedance monitoring, piezoceramics, ultrasound.

INTRODUCTION

Needle aspiration biopsy is a diagnostic procedure used to investigate thyroid, breast, liver and lung cancer amongst others [1]. Although percutaneous biopsies are generally safe, potential risks include the deposition of viable tumor cells along the needle tract, and post biopsy hemorrhage [2-3]. Cauterization of needle tracts is known to minimize these risks. Radio frequency (RF) ablation of biopsy needle tracts for this purpose has been reported in [4-5]. Cauterization of the needle tract using array of 200 µm-diameter lead zirconate titanate (PZT) transducers integrated at the tip of a 20-gauge biopsy needle has been discussed in [6].

One potential risk with any cauterization method is the possibility of excessive damage to surrounding healthy tissue. It is desirable to be able to detect the extent of tissue cauterization. Here, we describe the experimental results on monitoring the tissue ablation using changes in the electromechanical impedance characteristics of the PZT-embedded cauterization tools (Fig. 1). This capability, along with previously-reported tissue-contrast detection for needle-tip-positioning guidance [7] will provide, in the long term, a servo-controlled solution for biopsy and needle-tract cauterization of targeted tissue. The following sections present the analytical model for predicting the changes in the impedance characteristics of PZT due to cauterization; device description and fabrication; and the experimental results on the cauterization monitoring using the proposed method.

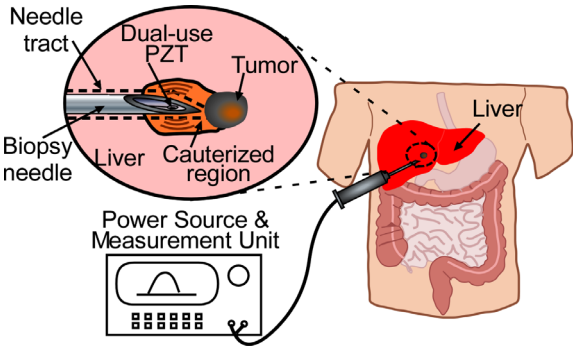

Figure 1: Conceptual diagram of a biopsy needle with an integrated PZT transducer for cauterization and detecting the extent of cauterization of the surrounding tissue.

THEORY AND ANALYTICAL MODEL

The resonance frequency and magnitude of the electromechanical impedance of a PZT-embedded structure depend on the density, elastic modulus and loss factor of the surrounding medium. The elastic modulus and loss factor in the tissue increases after ablation, thereby providing a method for monitoring tissue cauterization [8]. A modified Butterworth-Van-Dyke circuit model (Fig. 2) is used to predict the variation in impedance characteristics of the PZT in air, and in tissue before and after cauterization [9,10]. The circuit includes a static branch (C_0) and infinite number of

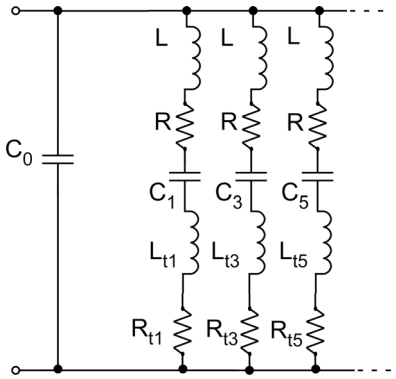

Figure 2: Modified Butterworth Van Dyke (BVD) equivalent circuit for predicting the frequency shift in resonance due to tissue cauterization.

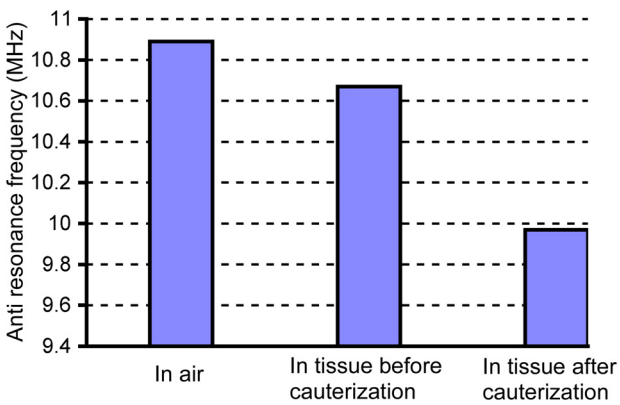

Figure 3: Analytical modeling results for the variation of anti-resonance frequency when the biopsy needle tip is in air, and in tissue before and after cauterization.

motional branches (R, L, C_n) connected in parallel, with each motional branch corresponding to different resonance modes. The various resistors, capacitors and inductors in the circuit are [7,9]:

$$C_0 = \frac{\varepsilon A}{t_0}, \quad L = \frac{1}{4\pi^2 f_{a1}^2 C_1}, \quad C_n = \frac{8k_t^2/n^2\pi^2}{1-8k_t^2/n^2\pi^2}C_0, \quad R = \frac{\eta_0}{\rho_0 v_0^2 C_1}\left(\frac{f}{f_{a1}}\right) \quad (1)$$

where k_t is the electro-mechanical coupling constant, η_0 is the viscosity of PZT layer, ρ_0 is the density of PZT, A is the area of PZT, v_0 is the acoustic velocity in PZT, t_0 is the PZT thickness and ε is the dielectric permittivity in PZT. The resonance frequency, f_{rn} (at minimum impedance), and the anti-resonance frequency, f_{an} (at maximum impedance), are given by:

$$f_{an} = \frac{1}{2\pi\sqrt{LC_n}}, \quad f_{rn} = \frac{1}{2\pi\sqrt{LC_n\dfrac{C_0}{C_0 - C_n}}} \quad (2)$$

Table 1. Material properties used in the BVD analytical model.

Normal tissue [9]	
Density, ρ_t	1054 kgm^{-3}
Storage modulus, G'	5500 Pa
Loss factor, η	13 Pa.s
Cauterized tissue [9]	
Storage modulus, G'	37000 Pa
Loss factor, η	230 Pa.s
PZT-5A	
Young's modulus, E_0	5.2x10^{10} Pa
Density, ρ_0	7800 kgm^{-3}
Coupling constant, K_t	0.72
Relative dielectric constant	1800

The effect of tissue loading is modeled by adding the resistor R_{tn} and inductor L_{tn} to the motional branches of the circuit. For a semi-infinite viscoelastic medium R_{tn} and L_{tn} are given by [10]:

$$R_{tn} = \frac{n\pi}{4k_t^2\omega C_0 Z_q}\left[\frac{\rho_t\left(|G|+G'\right)}{2}\right]^{0.5}, \quad L_{tn} = \frac{n\pi}{4k_t^2\omega^2 C_0 Z_q}\left[\frac{\rho_t\left(|G|-G'\right)}{2}\right]^{0.5} \quad (3)$$

where $G = G' + i\eta\omega$, $Z_q = \sqrt{E_0\rho_0}$, E_0 is the young's modulus of PZT, ρ_t is the tissue density, ω is the operation frequency, G' is the tissue storage modulus, η is the loss factor in tissue and Z_q is the PZT acoustic impedance. Table 1 lists the material properties used in the model. The fundamental anti-resonance frequency, which is the mode to be used for experiments, when the biopsy needle tip is in air, and in tissue before cauterization and after cauterization, is shown in Fig. 3. Analytical modeling results suggest that the fundamental anti-resonance frequency decreases by 0.65 MHz after cauterization.

DEVICE DESCRIPTION AND FABRICATION

The schematic of the proposed device is shown in Figure 4a. The PZT discs (diameter = 200 µm; thickness ≈ 100 µm) were batch-fabricated using micro ultrasonic machining process (µUSM) [11]. The µUSM tools were fabricated from stainless steel using micro electro-discharge machining (µEDM). The pattern on the tool was then transferred to the PZT-5A plate using µUSM with fine tungsten carbide slurry. The patterned PZT discs were released by lapping from the back side. Finally, Ti/Au layers were sputtered to form the electrodes. The sides of the discs were covered with a thin layer of photoresist to prevent shorting of the two electrodes during sputtering.

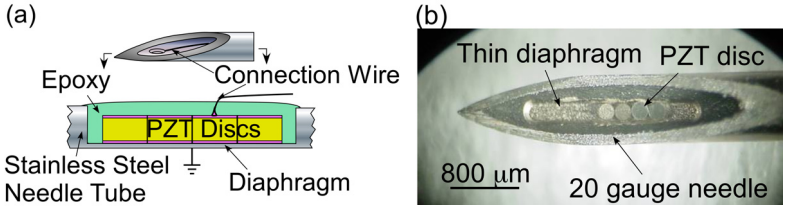

Figure 4: (a) Schematic and (b) photograph of a 20-gauge biopsy needle with four PZT discs integrated into a slot at its tip.

Figure 4b shows the photograph of the PZT discs integrated into a slot at the tip of a needle. This prevented the discs from blocking the path for acquiring tissues during the biopsy process. Flexible copper wire within the needle lumen provided power to the top electrode while the needle body provided the ground return path.

EXPERIMENTAL RESULTS

The experiments were conducted by inserting the biopsy needle into a porcine tissue sample (Fig. 5). The porcine tissue sample was cauterized by actuating the PZT discs with an RMS voltage of 14 V at its fundamental anti-resonance frequency of 9.6 MHz. Figure 5 shows the section view of the needle tip inserted in fresh porcine tissue before cauterization and the top-view of the cauterized tissue. The impedance characteristics of the PZT discs were measured using an Agilent 4395A impedance analyzer. All impedance measurements were conducted at room temperature unless stated otherwise.

Figure 6 shows the variation of the impedance characteristics of the PZT transducer for the following three cases: biopsy needle tip in air, and in tissue before and after cauterization. The fundamental anti-resonance frequency (f_{a1}) of the PZT discs was used for monitoring of cauterization. When the biopsy needle was inserted into the tissue, f_{a1} dropped from 9.66 MHz to 9.61 MHz. After cauterization, f_{a1} and the peak impedance magnitude further decreased by 0.6

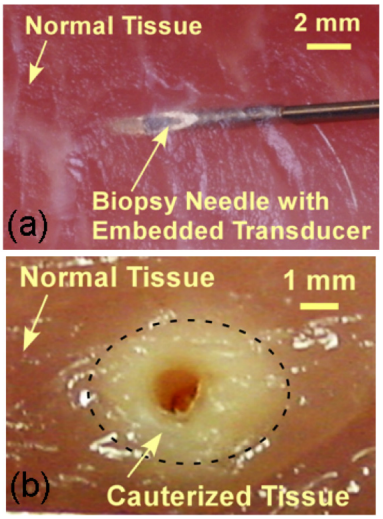

Figure 5: Photographs of: (a) the biopsy needle inserted into porcine tissue before cauterization; (b) porcine tissue after cauterization.

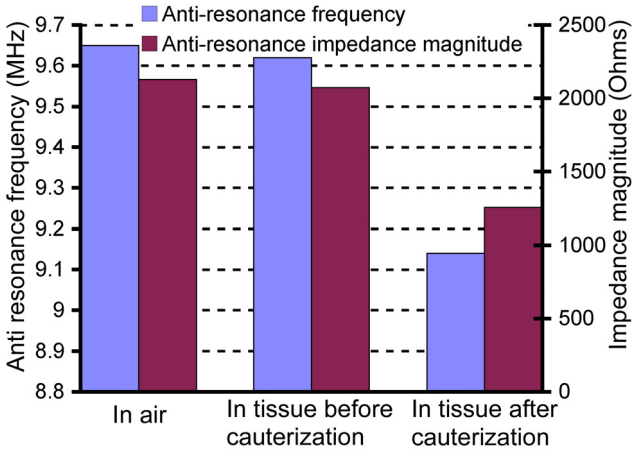

Figure 6: Measured variation, using Agilent 4395A impedance analyzer, of anti-resonance frequency and peak impedance magnitude, when the needle was in air, in tissue before and after cauterization (all at room temperature).

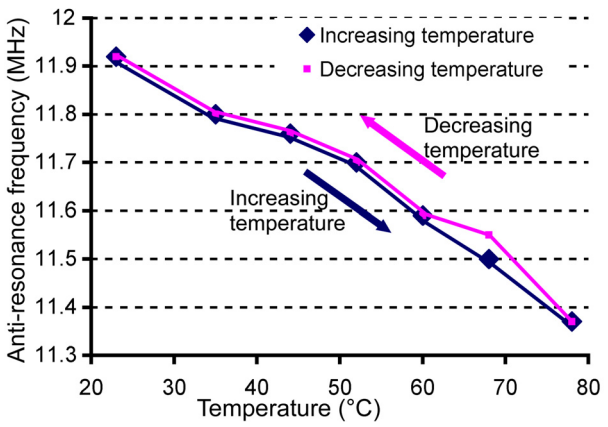

Figure 7: Measured variation of anti-resonance frequency with temperature in the range used for cauterization. The f_{a1} returned to the original value at the range of temperatures from body temperature to room temperature.

MHz and 900 ohms, respectively (Fig. 6). This decrease matches to that predicted by the analytical model and can be used to monitor the progress of cauterization.

The variation in f_{a1} was also measured with temperature varied in the range for cauterization while the needle tip stayed in air. Even though f_{a1} decreased (from 11.92 MHz to 11.38 MHz) with increasing temperature (from 22°C to 78°C), it was observed that f_{a1} returned to its initial value when the needle was cooled down to room temperature (Fig.7). As the readings in Fig. 6 were all made at the same room temperature, additional correction is not necessary.

CONCLUSION

The use of variations in the impedance characteristics of the PZT embedded biopsy needle for *in-situ* monitoring of biological tissue cauterization is discussed. An analytical model based on modified Butterworth-Van-Dyke circuit model is used to predict the variation of the resonance frequency due to cauterization. Cauterization of porcine tissue sample results in a decrease of 0.6 MHz in the resonance frequency and 900 ohms in the peak impedance magnitude, thereby providing a way to monitor the extent of cauterization. This approach bears significant promise in the long term for developing miniaturized servo-controlled cauterization procedure.

ACKNOWLEDGEMENTS

This work was supported in part by a fellowship to K. Visvanathan from the UM Mech. Eng. Dept.

REFERENCES

[1] R.G. Amedee, N. R. Dhurandhar, "Fine needle aspiration biopsy," *The Laryngoscope,* 111, pp.1551-1557, 2001.

[2] A. Pelloni, P. Gertsch., "Risks and consequences of tumor seeding after percutaneous fine needle biopsy for diagnosis of hepatocellular carcinoma," *Schweiz Med Wochenschr,* 130, pp. 871–877, 2000.

[3] S S. Sugano, Y. Sumino, T. Hatori, H. Mizugami, T. Kawafune, T. Abei, "Incidence of ultrasound-detected intrahepatic hematomas due to Tru-cut needle liver biopsy," *Digest. Dis. Sci.,*36, pp.1229–33, 1991.

[4] S. A. Dromi, J. Locklin, B. J. Wood, "Radiofrequency cauterization: an alternative to reduce post-biopsy hemorrhage," *Cardiovasc. Inter. Rad.,* 28, pp. 681-682, 2005.

[5] W.F. Pritchard, D. W. Cahen, J. W. Karanian, S. Hilbert, B. J. Wood, "Radiofrequency cauterization with biopsy introducer needle," *J Vasc Interv. Radiol.,* 15, pp. 183-187, 2004.

[6] K. Visvanathan, Y. B. Gianchandani, ,"Biopsy needle tract cauterization using an embedded array of piezoceramic microheaters," *IEEE Intl. Conf. MEMS,* pp. 987-1000, 2010.

[7] T. Li, R. Y. Gianchandani, Y. B. Gianchandani, "Micromachined bulk PZT tissue contrast sensor for fine needle aspiration biopsy," *Lab Chip*, 7, pp. 179-185, 2007.

[8] M. Z. Kiss, T. Varghese, T. J. Hall, "Viscoelastic characterization of *in vitro* canine tissue," *Phys. Med. Biol.,* 49, pp. 4207-4218, 2004.

[9] W. Pan, P. Soussan, B. Nauwelaers, H. A. C. Tilmans, "A surface micromachined electrostatically tunable film bulk acoustic resonator," *Sensors and Actuators A,* 126, pp. 436-446, 2006.

[10] H. L. Bandey, S. J. Martin, R. W. Cernosek, "Modeling the responses of thickness-shear mode resonators under various loading conditions," *Anal. Chem.,* 71, pp. 2205-2214, 1999

[11] T. Li, Y. B. Gianchandani, "A micromachining process for die-scale pattern transfer in ceramics and its application to bulk piezoelectric actuators," *J. Microelectromechanical Sys.,* 15, pp. 605-12, 2006.

CONTACT

*K. Visvanathan, tel: +1-734-846-3450; vkarthik@umich.edu